



## **Fiber-matrix integrity, micromorphology and flexural strength of glass fiber posts: Evaluation of the impact of rotary instruments**

Pereira, Gabriel Kalil Rocha ; Lançanova, Mateus ; Wandscher, Vinicius Felipe ; Kaizer, Osvaldo Bazzan ;  
Limberger, Inácio ; Özcan, Mutlu ; Valandro, Luiz Felipe

**Abstract:** Several rotary instruments have been daily employed on clinic to promote cut aiming to adjust the length of fiber posts to the radicular conduct, but there is no information on the literature about the effects of the different rotary instruments and its impact on the micromorphology of surface and mechanical properties of the glass fiber post. This study aimed the impact of rotary instruments upon fiber-matrix integrity, micromorphology and flexural-strength of glass-fiber posts (GFP). GFP (N=110) were divided into 5 groups: Ctrl: as-received posts, DBc: coarse diamond-bur, DBff: extra-fine diamond-bur, CB: carbide-bur, DD: diamond-disc. Cutting procedures were performed under abundant irrigation. Posts exposed to rotary instruments were then subjected to 2-point inclined loading test (compression 45°) (n=10/group) and 3-point flexural-strength test (n=10/group). Fiber-matrix integrity and micromorphology at the cut surface were analyzed using a SEM (n=2/group). Cutting procedures did not significantly affect the 2-point (51.7±4.3-56.7±5.1 MPa) (p=0.0233) and 3-point flexural-strength (671.5±35.3-709.1±33.1 MPa) (p=0.0968) of the posts (One-way ANOVA and Tukey's test). Fiber detachment was observed only at the end point of the cut at the margins of the post. Cut surfaces of the CB group were smoother than those of the other groups. After 3-point flexural strength test, fiber-matrix separation was evident at the tensile side of the post. Rotary instruments tested with simultaneous water-cooling did not affect the resistance of the tested fiber posts but caused disintegration of the fibers from the matrix at the end of the cut, located at the margins.

DOI: <https://doi.org/10.1016/j.jmbbm.2015.04.008>

Posted at the Zurich Open Repository and Archive, University of Zurich

ZORA URL: <https://doi.org/10.5167/uzh-116035>

Journal Article

Accepted Version



The following work is licensed under a Creative Commons: Attribution-NonCommercial-NoDerivatives 4.0 International (CC BY-NC-ND 4.0) License.

Originally published at:

Pereira, Gabriel Kalil Rocha; Lançanova, Mateus; Wandscher, Vinicius Felipe; Kaizer, Osvaldo Bazzan; Limberger, Inácio; Özcan, Mutlu; Valandro, Luiz Felipe (2015). Fiber-matrix integrity, micromorphology and flexural strength of glass fiber posts: Evaluation of the impact of rotary instruments. *Journal of the Mechanical Behavior of Biomedical Materials*, 48:192-199.

DOI: <https://doi.org/10.1016/j.jmbbm.2015.04.008>

**Category of manuscript: Original**

Title:

**Impact of rotary instruments upon fiber-matrix integrity, micromorphology and flexural strength of glass fiber posts**

Gabriel Kalil Rocha PEREIRA<sup>1</sup>, Mateus LANCANOVA<sup>1</sup>, Vinicius Felipe WANDSCHER<sup>1</sup>, Osvaldo Bassan KAIZER<sup>1</sup>, Inácio Fontoura LIMBERGER<sup>2</sup>, Mutlu ÖZCAN<sup>3</sup> and Luiz Felipe VALANDRO<sup>1</sup>

*<sup>1</sup>Department of Restorative Dentistry, Faculty of Dentistry, Federal University of Santa Maria, Brazil*

*<sup>2</sup>Department of Mechanical Engineering, Faculty of Mechanical Engineering, Federal University of Santa Maria, Brazil*

*<sup>3</sup>Dental Materials Unit, Center for Dental and Oral Medicine, Clinic for Fixed and Removable Prosthodontics and Dental Materials Science, University of Zürich, Plattenstrasse 11, CH-8032 Zürich, Switzerland*

**Keywords:** Fiber post, Fiber reinforced composite, Flexural strength, Root post, Rotary instruments

Numbers of reprints: 50

*Corresponding author, Luiz Felipe VALANDRO; Email: [lfvalandro@hotmail.com](mailto:lfvalandro@hotmail.com)*

*Tel: (55) 55-3220-9276, Fax: (55) 55-3220-927*

## **ABSTRACT**

This study assessed the impact of rotary instruments upon fiber-matrix integrity, micromorphology and flexural strength of glass fiber posts (GFP). Glass fiber posts (N=110) were divided into 5 groups: Ctrl: As-received posts, DBc: Coarse diamond bur, DBff: Extra-fine diamond bur, CB: Carbide bur, DD: Diamond disc. Cutting procedures were performed under abundant irrigation. Posts exposed to rotary instruments were then subjected to 2-point (compression 45°) (n=10/group) and 3-point flexural strength (n=10/group). Fiber-matrix integrity and micromorphology at the cut surface were analyzed using a Scanning Electron Microscope (n=2/group). Cutting procedures did not significantly affect the 2-point ( $51.7 \pm 4.3$  -  $56.7 \pm 5.1$  MPa) ( $p=0.0233$ ) and 3-point flexural strength ( $671.5 \pm 35.3$  -  $709.1 \pm 33.1$  MPa) ( $p=0.0968$ ) of the posts (One-way ANOVA and Tukey's test). Fiber detachment was observed only at the end point of the cut at the margins of the post. CB cut surfaces was smoother than those of the other groups. After 3-point flexural strength test, fiber-matrix separation was evident at the tensile side of the post.

## INTRODUCTION

Endodontically treated teeth that have lost a great portion of coronal structure often require intraradicular anchoring to retain the reconstruction material<sup>1)</sup>. The choice of a suitable material for intraradicular retainers is still controversial and generates discussion in the dental community<sup>2-6)</sup>. In addition to retention, one of the important requirements of intraradicular retainers is their effect in terms of homogeneous distribution of stress on the restored assembly. Accordingly, fiber reinforced composite (hereon: fiber) posts seem to better fulfill this biomechanical aspect, as they have a Young's modulus similar to dentin<sup>1,3-5)</sup>. The fact that these materials are also more biomechanically compatible also contributes to reduce the risk of root fracture<sup>6-8)</sup>.

The flexural properties of the fiber posts are influenced by the type, percentage, diameter<sup>9)</sup>, and quantity of the fibers<sup>10)</sup>. Rigidity and strength of the fiber posts are strongly linked to the polymer matrix and type of reinforcing fiber polymer<sup>9)</sup>. On the other hand, the reinforcing capacity of the fibers is based on their orientation, diameter, bonding to the polymer matrix, and impregnation to the matrix<sup>10)</sup>.

From the clinical point of view, a part of the crown portion of pre-fabricated fiber posts should be cut when used as intraradicular retainers. This cutting procedure may affect the strength of the posts, since it may have some impact on their integrity, damaging the bond between fibers and resin matrix<sup>11)</sup>. The bonding of fibers to the polymeric matrix is a factor of great importance for the resistance of the posts. This adhesion might be influenced by a process of controlled pre-industrial silanization of glass fibers that provides better chemical bonding of the fibers (inorganic material) to the organic matrix<sup>12,13)</sup>. The mechanical characteristics and performance of resin composite materials greatly increase when the bond between the inorganic filler and the organic matrix has been optimized<sup>14)</sup>. As a consequence, the resistance of fiber posts can be affected, which may have significant clinical consequences, including the fracture of fiber posts, catastrophic failure of the restoration or loss of retention of the root post.

There is limited information in the literature regarding the effect of cutting fiber post and the integrity of fiber-reinforced polymers when using different rotary instruments<sup>11)</sup>. Thus, the objectives of this study were

a) to assess the impact of rotary instruments upon fiber-matrix integrity, 2-point and 3-point flexural strength and b) to study the surface micromorphology after cutting procedures. The null hypothesis tested was that the various rotary instruments used for cutting fiber posts would not affect their flexural strength.

## **MATERIALS AND METHODS**

### *Experimental design and specimen preparation*

Double-tapered fiber posts (N=60) (White Post DC #3, FGM, Joinville, SC, Brazil; coronal diameter: 2 mm, apical diameter: 1.25 mm, length: 20 mm) were used for the 2-point flexural test. Cylindrical fiber posts (N=60) (20 mm x 2 mm), exclusively fabricated for this investigation by the same manufacturer with the same composition as the double-tapered fiber posts, were utilized for the 3-point flexural test.

For the 2-point flexural strength test, posts (n=10/group) were embedded in acrylic resin (Vipi, Pirassununga, SP, Brazil). They were marked with graphite at 10 mm from the apical aspect, measured using a digital caliper, coupled to an adapted surveyor to ensure parallelism to the vertical plan, and embedded in acrylic resin in PVC cylinders ( $\varnothing$ = 25 mm x h=14 mm) until the marking (10 mm inside the acrylic resin). After acrylic resin polymerization, the level to be cut was marked (5 mm above the acrylic resin) and the sectioning was performed for each group, with the exception for posts fabricated by the manufacturer having a length of 15 mm constituting the control group.

For the 3-point flexural strength test, the cylindrical fiber posts (n=10) were previously marked by graphite at 15 mm with the aid of a digital caliper (Starrett 727, Starrett, Itu, SP, Brazil). Subsequently, a single calibrated operator blinded to the objectives of this study performed a manual sectioning of the specimens at the marking, using cutting instruments as described below, with the exception of the control group.

The fiber posts were assigned randomly according to the rotary instruments (Table 1):

CTRL: Control group, as received fiber posts were not exposed to any cutting procedure. For the 2-point flexural test, 10 fiber posts with a length of 15 mm were produced by the manufacturer, since the posts were not cut, they had the same length as the fiber posts from the other groups after those posts had been

cut.

DBc: Coarse diamond bur (3216 KG Sorensen, Cotia, SP, Brazil)

DBff: Extra-fine diamond bur (3216FF KG Sorensen)

CB: Carbide bur (558 KG Sorensen)

DD: Diamond disc (double-sided, Ø= 22 mm, thickness= 0.1 mm, ref. 7020; KG Sorensen).

Cutting in groups DBc, DBff, and CB were performed at high speed (Kavo Extra Torque 605C – 380.000 rpm, Kavo Factory Ind. Ltd., Joinville, SC, Brazil), while group DD was sectioned with a handpiece at low speed (Kavo handpiece INTRAmatic ABN 10 181 1:1 and Micromotor INTRAmatic DBN – 20.000 rpm, Kavo Factory Ind.). All of the cutting procedures were performed under water-cooling.

#### *Two-point flexural strength test (compression at 45°)*

Specimens (fiber posts embedded in the acrylic resin) were placed at 45° relative to the horizontal plane (Fig. 1a) in the Universal Testing Machine (EMIC DL 2000, Sao Jose dos Pinhais, PR, Brazil) and a metallic jig induced load at a speed of 1 mm/min to the incisal surface of the post until fracture of the specimen. The stress ( $\tau$  in MPa) at the moment of fracture was calculated using the following formula:

$$\tau = 16.F_{max}.\cos 45 / 3.\pi.D^2$$

Where,  $F_{max}$  = Maximum force (N) for fracture of the specimen;  $\cos 45$  = cosine of the angle 45° (in this case,  $F_{max}.\cos 45$  refers to the component  $F_y$  of the original  $F_{max}$ , Figs. 2a-b),  $\pi = 3.14$ ;  $D$  = Diameter (= 2 mm) of the specimen at the deflection point (fulcrum).

#### *Three-point flexural strength test*

The cylindrical fiber posts were tested in the Universal Testing Machine (EMIC DL 2000) according to ISO 10477:1992<sup>9,11,14,15</sup> (Fig. 1b). The 3-point flexural strength test ( $\sigma$  in MPa) was calculated using the following formula:

$$\sigma = 8.F_{max}.L / \pi.D^3$$

Where  $F_{max}$  = Maximum force (N) applied for the fracture of the specimen;  $L$  = distance (in mm) between the lower supports (span), in this study a 10 mm span was used;  $\pi = 3.14$ ;  $D$  = Diameter of the specimen

(2 mm) (Fig. 3)<sup>14-16</sup>.

#### *Micromorphological analysis*

Additional double-tapered fiber posts (n=2 per group) were used for the micromorphologic analysis. They were cut as described above, cleaned ultrasonically (1440 D Odontobras, Ribeirão Preto, SP, Brazil) in distilled water for 10 minutes and air-dried.

For the scanning electron microscope (SEM) (JSM-6360, JEOL, Japan) analysis, the fiber posts were fixed on a metal base, with the cross section positioned upward, and gold sputtered (Denton Vacuum, DESK II, Beijing, China). The surface analyses were performed under x45 and x150 magnifications.

#### *Statistical analysis*

Statistical analysis were made using Statistix 8.0 for Windows (Analytical Software Inc, Tallahassee, FL, USA). One-way analysis of variance (ANOVA) was used to determine the significant differences between cutting groups after 2-point and 3-point flexural strength tests. The multiple comparisons were performed using a post-hoc Tukey's test. P values less than 0.05 were considered to be statistically significant in all tests.

## **RESULTS**

Cutting procedures did not significantly affect the 2-point ( $51.7 \pm 4.3$  -  $56.7 \pm 5.1$  MPa) ( $p=0.0233$ ) and 3-point flexural strength ( $671.5 \pm 35.3$  -  $709.1 \pm 33.1$  MPa) ( $p=0.0968$ ) of the posts (One-way ANOVA and Tukey's test) (Table 2).

The majority of the specimens after 2-point flexural strength test showed crack formation in the long axis of the specimen and separation of the fiber from the matrix. After 3-point flexural strength test, fiber-matrix separation was evident at the tensile side of the post (Figs. 4a-d).

Fiber detachment was observed only at the end point of the cut at the margins of the post. CB cut surfaces was smoother than those of the other groups (Figs. 5a-b). Specimens of the control group (Ctrl) presented fibers completely embedded in the polymer matrix, showing a regular cut made by the

manufacturer, with no apparent flaws on the surface whereas other groups showed separation of fibers from matrix at the end point of the cut (Figs. 5c-l).

## DISCUSSION

The results of the present study showed that the effect of cutting glass fiber posts, irrespective of the type of rotating instruments according to both type of tests, were unable to promote any structural changes that might adversely affect the flexural strength of fiber posts.

Although some detachment of fibers from the polymer has been observed in the final portion of the cut, this detachment was found to be insufficient to interfere with the 2-point and 3-point flexural strength results. These findings could indicate suitable quality of the composite material tested. Yet, additional studies for predicting the long-term effect of the cutting methods tested (mechanical cycling) are necessary. It is important to note that when the post was cut after cementation and resin core reconstruction, composite resin around the post promoted a protective effect and prevented the detachment of fibers. The lowest granulation of the DBff bur generated greater friction during cutting, which may have caused a greater displacement of fibers at the final portion of the section. The cut when using carbide burs created a surface with different cutting planes because of the inherent characteristics of the cutting tool as a multi-laminated bur.

The material tested is classified as a composite produced by combining two or more distinct components to form a new material with improved properties. The most common engineering composites are composed of strong fibers retained by a matrix<sup>17,18)</sup>. Some important factors influencing the mechanical properties of the fiber posts include intrinsic properties, such as the elastic and flexural moduli, surface treatment of the fibers and their impregnation in resin, bonding between the fibers and the matrix, the fiber density<sup>9)</sup>, diameter, orientation, position<sup>8-19)</sup>, and water absorption by the matrix<sup>9,18)</sup>. One of the most important chemical factors influencing the resistance of the post is related to the process of bonding between the fibers and the resin matrix. The mechanical characteristics and performance of composite



resins increased after improving the bond between the inorganic filler and the organic matrix<sup>14)</sup>. This bond improvement is created by applying a layer of silane to the inorganic material (fibers) in order to provide a better chemical bond to the organic matrix<sup>12-14)</sup>. Given this evidence, the type of resin matrix and the manufacturing process used to promote chemical bonding between fibers and resin may be one of the most important factors in the resistance of fiber posts<sup>14)</sup>. However, details of cutting procedures for the control group were not available by the manufacturers.

Clinically, cutting the fiber post is carried out prior to cementation and/or after core reconstruction<sup>11)</sup>. The factors characteristic to the fiber reinforced polymers, did not appear to have been affected by the methods tested, since the 2-point and 3-point flexural strengths did not change the results compared to the control group.

When considering micromorphological analysis, Grandini et al.<sup>11)</sup>, observed that the cut provided by a carborundum disk generated less regular surfaces when compared with diamond burs and presented burnt areas ("Burns"), probably caused by the absence of cooling during the cutting. However, those authors indicated that these factors were not sufficient to contraindicate their clinical use. In contrast, the specimens in the current study that were sectioned with a carbide disk presented a more regular surface, showing that water irrigation may be sufficient to promote a more homogeneous surface and prevent the formation of burnt areas (Burns).

Two-point<sup>2)</sup> and three-point<sup>16,20-22)</sup> flexural strength test have been extensively used to assess the mechanical properties (hardness, tensile, flexural modulus) of fiber reinforced polymeric materials used in dentistry. Therefore, these evaluation methods provide data that can be compared to the data from other studies. Failures from the 2-point test can be explained as a consequence of shear stresses within the specimen. When a fiber post is subjected to a load at 45°, it generates tensile, compression, and shear stresses<sup>23)</sup>. In order to understand these effects, the load on the specimen must be decomposed into a Cartesian axis, creating two vector components, X and Y. The component X causes only compressive stresses in the structure, which is uniformly distributed in the cross section, while the Y component leads to

the bending of the post. This bending generates tensile stresses at the lingual portion and compression stresses at the buccal portion, with maximum values at the specimen edges and minimum values at the center of the specimen<sup>24)</sup>. As a consequence of the Y component, shear stress occurs inside the post due to bending. Transverse loading causes stresses, although these stresses are minimum at the external portions and maximum at the center<sup>24)</sup>. Thus, the explanation for this failure is described as a function of the mechanical factors of loading in association with the fiber post composition. Since the post is basically composed of matrix and fiber, it is possible to conclude that the final fracture does not occur in the region exposed to tension due to the elasticity of these materials. Thus, the shear stress induces the separation of the fiber-matrix at the central portion of the post, where the shear is maximum. This type of failure is classified as “mode II in-plane shear, intralaminar”<sup>25)</sup>.

As the prevalent fracture in the current specimens basically was a consequence of shear stresses, the formula shown in Fig. 3 was used to calculate that stress. This formula is different from the one used by Asmussen et al.<sup>2)</sup>, which takes the original force "F" into consideration for calculating the bending stress. In order to calculate the tensile, compressive and shear stresses, the vector component  $F_y$ , from the original force F, should be used, since  $F_y$  is responsible for the bending of the specimen, causing tensile stress on the upper surface and compression on the lower surface, and shear stress being maximum on the neutral axis of the specimen. On the other hand, when considering the 3-point test, failure typically occurred on the surface opposite of the load application. This could be attributed to the characteristics of the polymer in question. The materials that comprise the fiber post are elastic upon the load application. Therefore, in the region where the force is applied (the central area of the specimen), the post undergoes a slight plastic deformation, becoming more elliptical in shape and presenting a crack on the opposite face due to "kneading" caused by the application of force. The failures in the current study were characterized as a fiber-to-matrix separation at the margins, and occurred as a consequence of the tensile stresses caused by "kneading". These failures are characterized as “mode I tension-intralaminar”<sup>25)</sup>.

One limitation of this current study is that the specimens were not aged by mechanical fatigue, which

can simulate clinical loading. Restorative materials fail more often under cyclic loading at lower values when compared to monotonic uniaxial loads<sup>8,25)</sup>. The mechanical fatigue loading could lead to the propagation of defects generated by cutting instruments, which could affect the strength of the fiber posts. Studies involving the cementing of posts in root canals to better simulate the clinical conditions should be conducted using mechanical fatigue to better predict the effects of the cutting methods<sup>26)</sup>.

It is also important to note that this study assessed a glass fiber reinforced polymer with a coronal diameter of 2 mm. It is possible that fiber posts with smaller diameters may have a different outcome, requiring further studies.

## **CONCLUSION**

Based on the results of this study, the following conclusions could be drawn:

1. Rotary instruments tested with simultaneous water-cooling did not affect the resistance of the tested fiber posts but caused disintegration of the fibers from the matrix at the end of the cut, located at the margins.
2. Failures after 3-point flexural test were mainly at the tensile side at the fiber-matrix interface.

## **ACKNOWLEDGMENTS**

This study financially was supported by the National Council for Research and Technology Developments (CNPq). The authors gratefully acknowledge FGM for providing the glass fiber posts. This work is based on the dissertation submitted to the Graduate School of Dentistry, Federal University of Santa Maria as part of the requirements for the DDS degrees of Gabriel Pereira and Mateus Lançanova.

## REFERENCES

1. Assif D, Gorfil C. Biomechanical considerations in restoring endodontically treated teeth. *J Prosthet Dent* 1994; 71: 565-567.
2. Asmussen E, Peutzfeldt A, Heitmann T. Stiffness, elastic limit, and strength of newer types of endodontic posts. *J Dent* 1999; 27: 275-278.
3. Vallittu PK. Flexural properties of acrylic resin polymers reinforced with unidirectional and woven glass fibers. *J Prosthet Dent* 1999; 81: 318-326.
4. Lanza A, Aversa R, Rengo S, Apicella D, Apicella A. 3D FEA of cemented steel, glass and carbon posts in a maxillary incisor. *Dent Mater* 2005; 21: 709-715.
5. Baldissara P, Zicari F, Valandro LF, Scotti R. Effect of root canal treatments on quartz fiber posts bonding to root dentin. *J Endod* 2006; 32: 985-988.
6. Monticelli F, Osorio R, Sadek FT, Radovic I, Toledano M, Ferrari M. Post-surface conditioning improves interfacial adhesion in post/core restorations. *Dent Mater* 2006; 7: 602-609.
7. Isidor F, Odman P, Brondum K. Intermittent loading of teeth restored using prefabricated carbon fiber posts. *Int J Prosthodont* 1996; 9: 131-136.
8. Ferrari M, Cagidiaco MC, Goracci C, Vichi A, Mason PN, Radovic I et al. Long-term retrospective study of the clinical performance of fiber posts. *Am J Dent* 2007; 20: 287-291.
9. Lassila LV, Nohrstrom T, Vallittu PK. The influence of short-term water storage on the flexural properties of unidirectional glass fiber-reinforced composites. *Biomater* 2002; 23: 2221-2229.
10. Obukuro M, Takahashi Y, Shimizu H. Effect of diameter of glass fibers on flexural properties of fiber-reinforced composites. *Dent Mater J* 2008; 27: 541-548.
11. Grandini S, Balleri P, Ferrari M. Scanning Electron Microscopic investigation of the surface of fiber posts after cutting. *J Endod* 2002; 28: 610-612.
12. Söderholm KJM, Shang SW. Molecular orientation of silane at the surface of colloidal silica. *J Dent Res* 1993; 72: 1050-1054.

13. Anusavise KJ, Phillips RW. Science of dental materials, 10th ed. Philadelphia: WB Saunders; 1996.
14. Galhano GA, Valandro LF, Melo RM, Scotti R, Bottino MA. Evaluation of the flexural strength of carbon fiber-, quartz fiber-, and glass fiber-based posts. J Endod 2005; 31: 209-211.
15. Lassila LV, Tanner J, Vallittu PK. Flexural properties of fiber reinforced root canal posts. Dent Mater 2004; 20: 29-36.
16. D'Arcangelo C, D'Amario M, Vadini M, De Angelis F, Caputi S. Influence of surface treatments on the flexural properties of fiber posts. J Endod 2007;33:864-867.
17. Barbero EJ. Introduction to composite materials design. 1st ed. Taylor and Francis, Philadelphia, 1999, p. xx-xx.
18. Dyer SR, Lassila LV, Jokinen M, Vallittu PK. Effect of fiber position and orientation on fracture load of fiber-reinforced composite. Dent Mater 2004; 20: 947-955.
19. Chung KH, Ling T, Wang F. Flexural strength of a provisional resin material with fibre addition. J Oral Rehabil 1998; 25: 214-217.
20. Ellakwa AE, Shortall AC, Shehata MK, Marquis PM. The influence of fibre placement and position on the efficiency of reinforcement of fibre reinforced composite bridgework. J Oral Rehabil 2001; 28: 785-791.
21. Abdulmajeed AA, Närhi TO, Vallittu PK, Lassila L. The effect of high fiber fraction on some mechanical properties of unidirectional glass fiber-reinforced composite. Dent Mater 2011; 27: 313-321.
22. Kim MJ, Jung WC, Seunghan OH, Hattori M, Yoshinari M, Kawada E et al. Flexural properties of three kinds of experimental fiber-reinforced composite posts. Dent Mater J 2011; 30: 38-44.
23. Hibbeler, RC. Mechanics of materials. 5th ed. São Paulo Pearson/Prentice Hall; 2006.
24. Beer FP, Johnston R Jr. Vector mechanics for engineers Statics. 5th ed. Makron Books do Brasil; 1994.
25. Smith TW, Grove RA. Failure Analysis Continuous Fiber Reinforced Composites. In: ASM Handbook Volume 11: Failure Analysis and Prevention. Shipley RJ and Becker WT (editors). Ohio: ASM International; 2002. p. 731-743.

26. Baldissara P, Özcan M, Melilli D, Valandro LF. Effect of cyclic loading on fracture strength and microleakage of a quartz fiber dowel with different adhesive, cement and resin core material combinations. *Minerva Stomatol.* 2010; 59: 407-414.

## Captions to the legends and tables

### Tables

**Table 1.** Experimental groups according to the rotary instruments used and the test methods.

**Table 2.** Mean, standard deviations (SD) (MPa) and coefficient of variation (CV) for 2-point flexural strength (Tukey's test) and 3-point flexural strength. Different capital letters in the same column indicate significant differences ( $p < 0.05$ ).

### Figures

**Figs. 1a-b** Experimental set up of **a)** 2-point, **b)** 3-point flexural strength test.

**Figs. 2a-b** **a)** Vectorial force acting upon the fiber post (original force at  $45^\circ$ ), **b)** Parallelogram law for calculating force vectors (Hibbeler 2006<sup>23</sup>), Beer & Johnston, 1991<sup>24</sup>), F: Original Force at  $45^\circ$ , HIP: hypotenuse, Fy: Vectorial component at Y axis, CO: opposite side to the angle, Fx: Vectorial component at X axis and CA: Adjacent side to the angle.

**Fig. 3** Representation of the Fy effects on the post structure. **C**: Compression, **T**: Tensile, **NL**: Neutral line,  $\sigma_x$ : Normal tension in X axis, **A**: Area, **M**: Static moment of area, **C**: Distance from neutral axis to the most forced position of the fiber, **I**: Inertia moment of the area, **t**: Thickness of cross-sectional area (post diameter),  $\tau$  = Shear stress, **V** = Load (in this case represented by the value of Fy), **Q** = Static moment of area, **I** = Moment of inertia of the area, **t** = Thickness of flat section.

**Figs. 4a-d** Representative images under stereomicroscope from the specimens submitted to 3-point flexural test. **a)** Note the compression zone at the load application point, **b)** the opposite side showing the failure, **c)** final failure at the center of the specimen, **d)** as a result of tensile stresses.

**Figs. 5a-l** Representative SEM micrographs of the cross-sectional the glass fiber post surfaces after cutting with different rotary tools (left to right: x45, x150, x150); **a-b)** Control; **c-d)** Coarse Diamond Bur; **e-f)** Extra-fine Diamond Bur; **g-h)** Carbide Bur; **i-j)** Diamond Disc. Note separation of the fiber from the matrix at the end of the cut (↗).

## Tables

N=110	Rotary Instruments	Experiments
	Control (Ctrl)	2-point flexural test (n=10)
		3-point flexural test (n=10)
		Micromorphology (n=2)
	Coarse Diamond Bur (DBc)	2-point flexural test (n=10)
		3-point flexural test (n=10)
		Micromorphology (n=2)
	Extra-fine Diamond Bur (DBff)	2-point flexural test (n=10)
		3-point flexural test (n=10)
		Micromorphology (n=2)
	Carbide Bur (CB)	2-point flexural test (n=10)
		3-point flexural test (n=10)
		Micromorphology (n=2)
	Diamond Disc (DD)	2-point flexural test (n=10)
		3-point flexural test (n=10)
		Micromorphology (n=2)

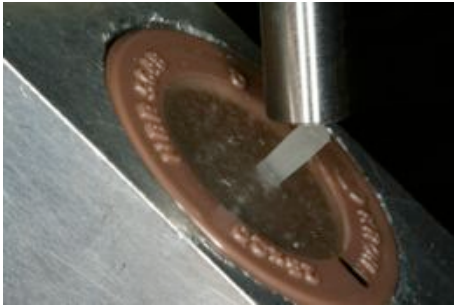
**Table 1.** Experimental groups according to the rotary instruments used and the test methods.

Experimental Groups	Means $\pm$ SD (CV)	
	2-point flexural test	3-point flexural test
Control	51.7 $\pm$ 4.3 <sup>B</sup> (18.54)	689.6 $\pm$ 31.1 <sup>A</sup> (4.50)
Coarse Diamond Bur	54.2 $\pm$ 3.3 <sup>AB</sup> (11.19)	709.1 $\pm$ 33.1 <sup>A</sup> (4.66)
Extra-fine Diamond Bur	54.8 $\pm$ 4.2 <sup>AB</sup> (17.73)	683.8 $\pm$ 25.3 <sup>A</sup> (3.69)
Carbide Bur	55.5 $\pm$ 4.2 <sup>AB</sup> (17.49)	671.5 $\pm$ 35.3 <sup>A</sup> (5.25)
Diamond Disc	56.7 $\pm$ 5.1 <sup>AB</sup> (26.43)	678.1 $\pm$ 31.1 <sup>A</sup> (4.59)

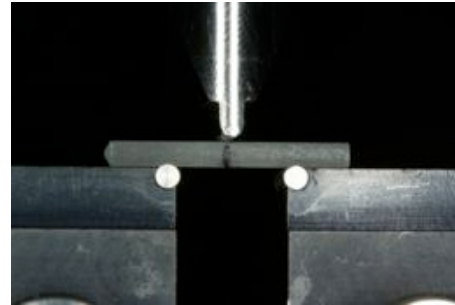
**Table 2.** Mean, standard deviations (SD) (MPa) and coefficient of variation (CV) for 2-point flexural strength (Tukey's test) and 3-point flexural strength. Different capital letters in the same column indicate significant differences ( $p < 0.05$ ).



## Figures

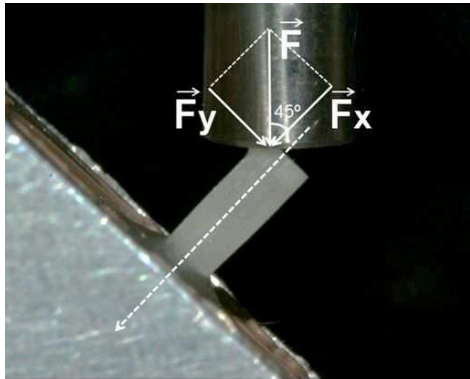


A

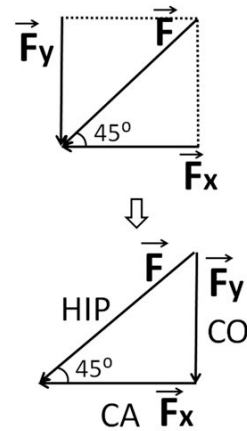


B

**Figures 1a-b.** Experimental set up of a) 2-point, b) 3-point flexural strength test.

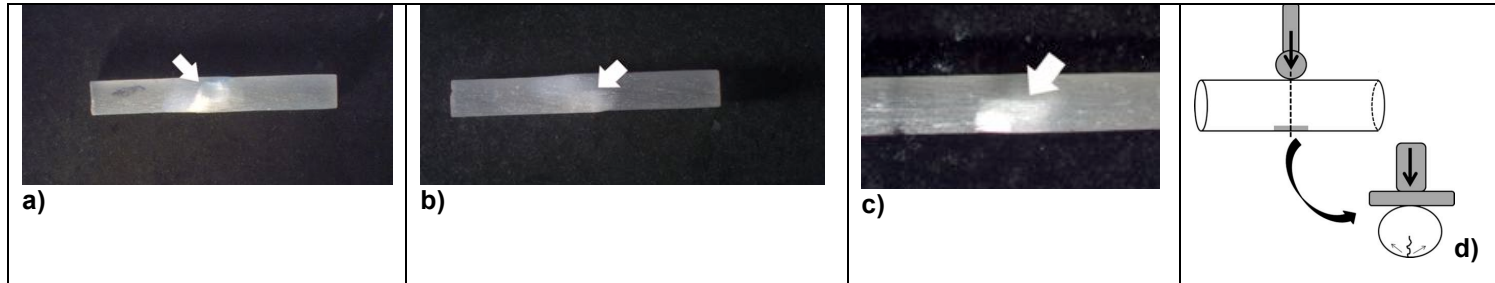


A



B

**Figures 2a-b.** a) Vectorial force acting upon the fiber post (original force at  $45^\circ$ ), b) Parallelogram law for calculating force vectors (Hibbeler 2006<sup>23</sup>), Beer & Johnston, 1991<sup>24</sup>), F: Original Force at  $45^\circ$ , HIP: hypotenuse, F<sub>y</sub>: Vectorial component at Y axis, CO: opposite side to the angle, F<sub>x</sub>: Vectorial component at X axis and CA: Adjacent side to the angle.



**Figures 3a-d.** Representative images under stereomicroscope from the specimens submitted to 3-point flexural test. **a)** Note the compression zone at the load application point, **b)** the opposite side showing the failure, **c)** final failure at the center of the specimen, **d)** as a result of tensile stresses.

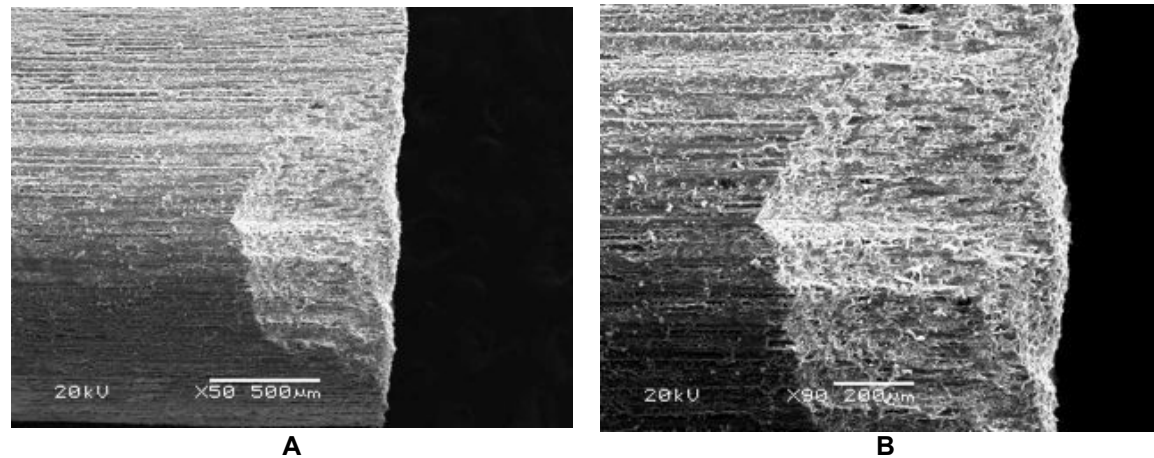
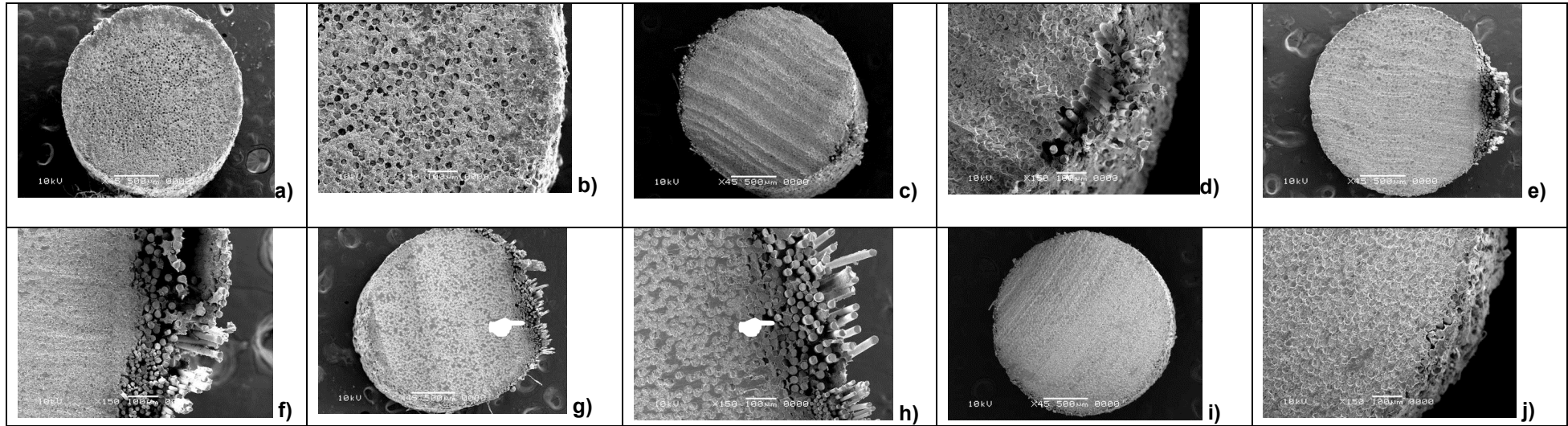


**Figure 4.** Representative micrographs (50x and 100x) from the end point of the cut at the margins of the post demonstrating that the defects introduced by grinding were restricted at this particular region of the post; it was not observed fiber detachment at the main body of the post.



**Figures. 5a-j** Representative SEM micrographs of the cross-sectional the glass fiber post surfaces after cutting with different rotary tools (left to right: x45, x150, x150); **a-b)** Control; **c-d)** Coarse Diamond Bur; **e-f)** Extra-fine Diamond Bur; **g-h)** Carbide Bur; **i-j)** Diamond Disc. Note separation of the fiber from the matrix at the end of the cut ( $\curvearrowright$ ).

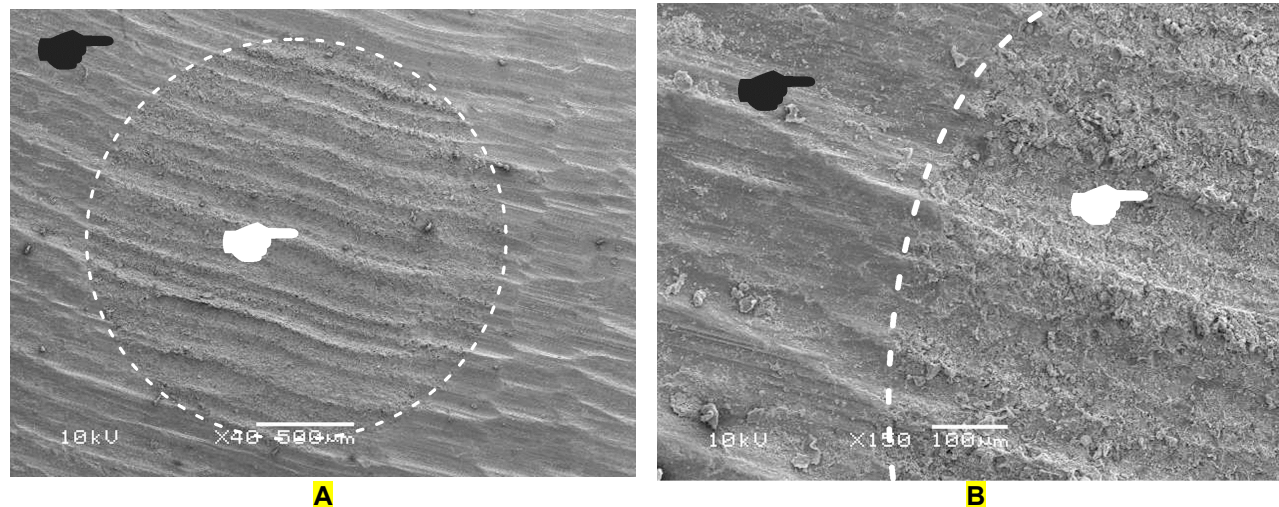


**Figure 6.** Representative micrographs from the cross-sectional surface of the glass fiber post and resin composite build-up after cutting with coarse diamond bur. The cut was made after the core reconstruction procedure with composite resin. The white-circle (A) and -line (B) correspond to the interface between resin composite ( $\blacktriangleright$ ) and fiber post ( $\curvearrowright$ ) approximately. It notes the protective effect for detachment of the glass fibers (none detachment of fibers from the matrix).

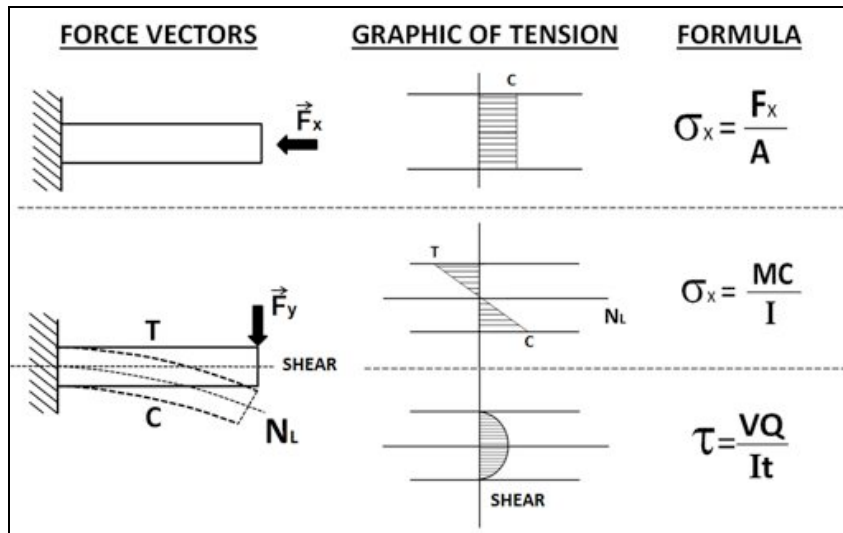


**Figure 7.** Representation of the  $F_y$  effects on the post structure. **C**: Compression, **T**: Tensile, **NL**: Neutral line,  $\sigma_x$ : Normal tension in X axis, **A**: Area, **M**: Static moment of area, **C**: Distance from neutral axis to the most forced position of the fiber, **I**: Inertia moment of the area, **t**: Thickness of cross-sectional area (post diameter),  $\tau$  = Shear stress, **V** = Load (in this case represented by the value of  $F_y$ ), **Q** = Static moment of area, **I** = Moment of inertia of the area, **t** = Thickness of flat section.